



HAL
open science

Frequency-selective surface acoustic invisibility for three-dimensional immersed objects

Mohamed Farhat, Pai-Yen Chen, Sébastien Guenneau, Stefan Enoch, Andrea
Alu

► **To cite this version:**

Mohamed Farhat, Pai-Yen Chen, Sébastien Guenneau, Stefan Enoch, Andrea Alu. Frequency-selective surface acoustic invisibility for three-dimensional immersed objects. *Physical Review B: Condensed Matter and Materials Physics (1998-2015)*, 2012, 86, pp.174303. 10.1103/PhysRevB.86.174303 . hal-00759739

HAL Id: hal-00759739

<https://hal.science/hal-00759739>

Submitted on 2 Dec 2012

HAL is a multi-disciplinary open access archive for the deposit and dissemination of scientific research documents, whether they are published or not. The documents may come from teaching and research institutions in France or abroad, or from public or private research centers.

L'archive ouverte pluridisciplinaire **HAL**, est destinée au dépôt et à la diffusion de documents scientifiques de niveau recherche, publiés ou non, émanant des établissements d'enseignement et de recherche français ou étrangers, des laboratoires publics ou privés.

Frequency Selective Surface invisibility for three dimensional immersed objects

Mohamed Farhat,^{1,2,*} Pai-Yen Chen,^{1,†} Sébastien

Guenneau,³ Stefan Enoch,³ and Andrea Alù^{1,‡}

¹*Department of Electrical and Computer Engineering,*

The University of Texas at Austin, Austin, TX, 78712, USA

²*Institute of Condensed Matter Theory and Solid State Optics,*

Abbe Center of Photonics, Friedrich-Schiller-Universität Jena, D-07743 Jena, Germany

³*Institut Fresnel, CNRS, Aix-Marseille Université,*

Campus universitaire de Saint-Jérôme, 13013 Marseille, France

(Dated: August 24, 2012)

Abstract

This paper is focused on the study of acoustic metasurface cloaking, based on the use of appropriate ultrathin pseudo-surfaces that may act as cloaking devices for a finite range of frequencies. The technique consists in tailoring the appropriate acoustic surface impedance which cancels the scattered field of a diffracting spherical obstacle placed in the trajectory of an impinging acoustical wave. Our numerical simulations of both near and far-fields show a significant reduction of scattering cross-section for a moderately broad range of frequencies, confirming the effectiveness of surface cloaks (easier to manufacture and less cumbersome than their bulk counterpart). We also go one step further by proposing a realistic structure obtained by quasi-periodically patterning the surface of a spherical layer. The effective properties of the metasurface are obtained in the framework of homogenization theory and confirm this realistic route to surface cloaking for acoustic waves.

I. INTRODUCTION

In 2006, Pendry *et al.* have shown that by surrounding a finite size object with a coating consisting of a metamaterial, it could be rendered transparent to electromagnetic radiation¹. The cornerstone of this work is a geometric transformation. Mimicking the heterogeneous and anisotropic nature of the permittivity and permeability tensors became possible only when Pendry suggested the use of newly discovered metamaterials. These are composite structures manufactured for their exotic properties enabling the control the electromagnetic field. A team lead by Pendry and Smith implemented this idea using a metamaterial consisting of concentric layers of Split Ring Resonators (SRRs), which made a copper cylinder invisible to an incident plane wave at 8.5 GHz as predicted by the numerical simulations². Independently and at the same time, Leonhardt studied conformal invisibility by solving the Schrodinger equation which is valid in the geometric optics limit^{3,4}. Parallel to these seminal studies, other methods have been investigated ranging from anomalous resonance of the so-called perfect lens⁵⁻⁷ to homogenization of quasi-photonic crystals to mimic anisotropy and space dispersion^{8,9}.

A different technique proposed back in 2005 by Engheta and Alù relies on matching the impedance of the surrounding media by canceling the scattering response of the object to be cloaked¹⁰. This method has the advantage of requiring homogeneous and isotropic cloaking shells unlike the transformation optics based cloaks. This allows one to think of practical realization of such devices for applications such as cloaking sensors¹¹, non-invasive imaging techniques through cloaking Scanning Optical Microscope Tip¹². Experimental evidence of such invisibility devices was demonstrated in the microwave regime¹³ and more recently in the 3D case¹⁴. More recently it has been proposed in Ref.¹⁵ to use clusters of silver nanoparticles as cloaking shells by arranging them in a random manner at the surface of dielectric spheres. In a cylindrical geometry a similar concept was investigated in Ref.¹⁶.

Different from metamaterial cloaking, objects may be made invisible also using a surface cloaking technology, as it was recently shown that a patterned meta-surface may produce similar cloaking effects in a simpler and thinner geometry¹⁷. Indeed, Alù and Chen proposed the surface cloaking technique¹⁸⁻²¹ based on scattering cancelation, in which an ultrathin mantle cloak with averaged surface reactance [frequency selective surface (FSS)²² or meta-surface] was shown to provide low visibility for moderately sized objects, comparable to the

one achievable with bulk metamaterial cloaks.

The acoustic counterpart was considered soon after. Cummer *et al.*²³ analyzed the $2D$ acoustic cloaking for pressure waves in a transversely anisotropic fluid by exploiting the analogy with TE electromagnetic waves. Torrent *et al.*²⁴ subsequently investigated this cloaking for concentric layers of solid lattices behaving as anisotropic fluids in the homogenization limit. Using a similar approach, Farhat *et al.*²⁵ independently demonstrated cloaking of surface liquid waves using a micro-structured metallic cloak which was experimentally validated at 10 Hz. Quite remarkably, Chen and Wu²⁶ and Cummer *et al.*²⁷ noticed that a $3D$ acoustic cloaking for pressure waves in a fluid can be envisaged since the wave equation retains its form under geometric changes. More recently, even a new class of acoustic cloaks based on the scattering cancellation technique^{28,29} and 2D FSS³⁰ were proposed.

In this paper, we build upon all these works and numerically demonstrate that acoustic cloaking may be achieved using ultrathin pseudo-surfaces for spherical pressure waves. The underlying mechanism is analogous to mantle cloaking for electromagnetic waves: a properly patterned meta-surface may support currents that may drastically reduce the scattering from a given object and thus suppressing its visibility. However, the governing equations are different. Moreover, we derive the homogenized parameters of the metasurface structure using a two-scale asymptotic expansion in the linearized acoustic equations. In the limit when the wavelength is much larger than the typical heterogeneity size of the quasi-phononic crystal, we show that it behaves as an artificial solid with an anisotropic effective shear modulus and an effective-mass density. The potential applications of this technology for a better control of acoustic waves open fascinating possibilities in achieving such invisibility for 3D (real-world) objects with light low profile meta-structures. We are also working on the extension of this principle to the domain of plate elasticity, where equations are also of fourth order and where applications such as anti-earthquake devices can be envisaged.

II. SETUP OF THE PROBLEM

The solutions to the Lamé equation for elastodynamics are pressure waves (longitudinal) and shear waves (transverse) that can be coupled in certain mediums. In this paper we limit our analysis to only pressure waves described by the classical $3D$ acoustic equation

$$\nabla \cdot (\tilde{\rho}^{-1} \nabla p) + \frac{\omega^2}{\kappa} p = 0 \quad (1)$$

with $\tilde{\rho}$ being the density rank-2 tensor of the fluid, κ its inhomogeneous bulk modulus, p the pressure field, and where we have assumed a time harmonic dependence $e^{-i\omega t}$.

The boundary conditions governing pressure discontinuity and the radial component of the velocity fields at the interface between the two mediums ($r > a_c$ and $a < r < a_c$) complete the setup of our problem (as can be seen in Fig. 1). Our aim is to show the possibility of drastically reducing the scattering from various spherical objects (e.g. hard and soft ones) by choosing the appropriate surface impedance (reactance), and to suppress their visibility.

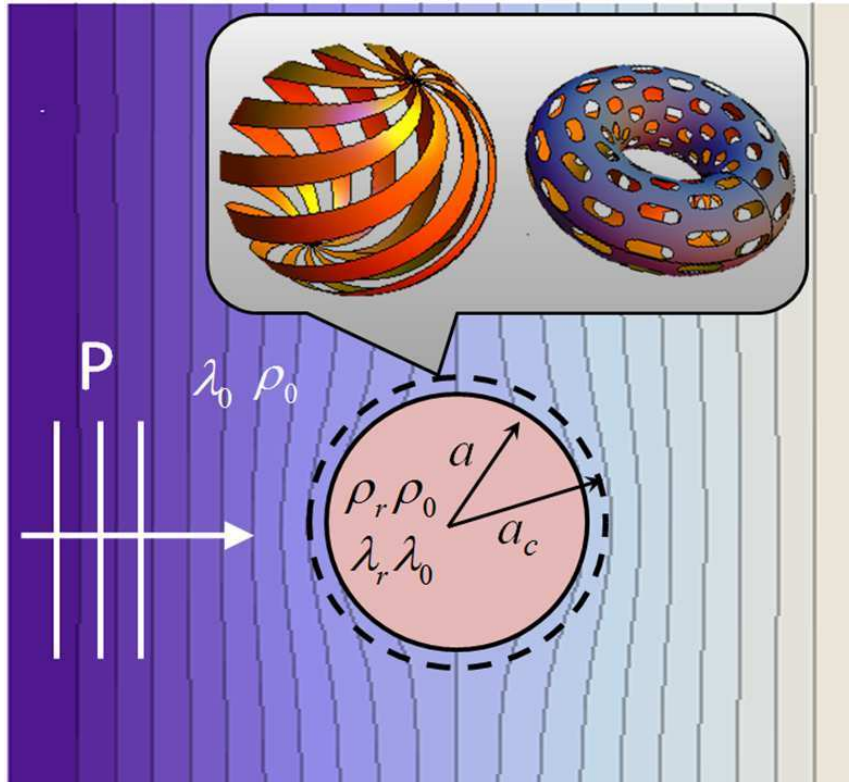


FIG. 1: Schematic of the cloaking mechanism: a metasurface of radius a_c is covering a sphere of radius a (2D view) are in the path of a plane pressure wave impinging from left. The mass density and bulk modulus inside the object (sphere of radius a) are respectively ρ_r, κ_r where ρ_0 is the density of the background and κ_0 its bulk modulus. The domain between $a < r < a_c$ is the same as the background medium, since our cloak (dashed line) is just an ultrathin surface with negligible thickness. The inset shows possible designs for acoustic FSS, including irregular shapes.

We consider a spherical object with radius a . We will denote with the suffix r all the acoustic properties relative to the scatterer, and by the suffix c the ones of the surface impedance, the free space will be referred by the suffix 0 (infinite acoustic medium where spherical waves are propagating).

The pressure field p is given in the different regions in form of Bessel expansions³¹, and the choice of the wave functions is dictated by the conditions that the scattered response is finite at $r = 0$ and must be outgoing, or radiating as $r \rightarrow \infty$.

The incident excitation is a plane wave of the form $e^{ik_0 r \cos \theta}$, where θ is the incidence angle, and can be expanded in spherical coordinates:

$$p^{\text{inc}} = P_0 \sum_{n=0}^{n=\infty} i^n (2n+1) j_n(k_0 r) P_n(\cos \theta) \quad (2)$$

where $P_n(\cos \theta)$ is the Legendre polynomial of order n and j_n denotes the n th spherical Bessel function [which is related to the ordinary Bessel function J_n through the relation $j_n(x) = \sqrt{\frac{\pi}{2x}} J_{n+1/2}(x)$]. P_0 is the amplitude of the incident field.

The radiation condition dictates the following form for the scattered field (in terms of spherical Hankel functions)

$$p^{\text{scatt}} = P_0 \sum_{n=0}^{n=\infty} c_n h_n^{(1)}(k_0 r) P_n(\cos \theta) \quad (3)$$

with $h_n^{(1)}(k_0 r)$ the spherical Hankel function of the first kind, and c_n are coefficients to be fixed by the boundary conditions.

There are two boundary conditions that should be satisfied at the surface of the spherical obstacle (on $r = a$) and the cloak ($r = a_c$). On the boundary $r = a$, we have only the continuity of the pressure and radial velocity, i.e., $p|_{r=a^-} = p|_{r=a^+}$, and $v_r|_{r=a^-} = v_r|_{r=a^+}$, where the signs $+$ ($-$) refer respectively to the inner (outer) region. In contrast, on the cloak boundary, we need to consider the acoustic surface impedance which produces a discontinuity of the normal velocity:

$$Z_s p|_{r=a_c} = v_r|_{r=a_c^+} - v_r|_{r=a_c^-}, \quad (4)$$

where we have used the continuity of the pressure field $p|_{r=a_c^-} = p|_{r=a_c^+} = p|_{r=a_c}$, and where $Z_s = R_s - iX_s$ is the averaged surface impedance that relates the pressure to the velocity

on the surface. This impedance is function only of the geometry of the structure and the wavelengths of the excitation signals and can usually vary over a large range of values.

The scattered far-field amplitude $f(\theta, \phi)$ is defined such that $p^{\text{scatt}} = \frac{1}{\sqrt{2r}} e^{i(k_0 r - \pi/4)} f(\theta, \phi) + o(1/\sqrt{r})$, $r \rightarrow \infty$. The scattering cross-section, σ^{scatt} , defined as the ratio of the scattered flux to the incident one, is an integration over the solid angle with incremental $d\Omega$:

$$\sigma^{\text{scatt}} = \frac{1}{2} \int d\Omega |f(\theta, \phi)|^2. \quad (5)$$

As a measure of the overall visibility of a given object Eq. (5) is given by the expression³¹

$$\sigma^{\text{scatt}} = \frac{2\pi}{|k_0|^2} \sum_{n=0}^{n=\infty} (2n+1) |c_n|^2, \quad (6)$$

where we can express $c_n = -P_n/(P_n + iQ_n)$. The n th spherical scattering harmonic can be suppressed provided that the following determinant is canceled (See Mie theory¹⁰)

$$P_n = \begin{vmatrix} j_n(k_r a) & j_n(k_0 a) & y_n(k_0 a) & 0 \\ k_r j'_n(k_r a) & k_0 j'_n(k_0 a)/\rho_0 & k_0 y'_n(k_0 a)/\rho_0 & 0 \\ 0 & j_n(k_0 a_c) & y_n(k_0 a_c) & j_n(k_0 a_c) \\ 0 & j'_n(k_0 a_c) - i\omega\rho_0 j_n(k_0 a_c)/(k_0 Z_s) & y'_n(k_0 a_c) - i\omega\rho_0 y_n(k_0 a_c)/(k_0 Z_s) & j'_n(k_0 a_c) \end{vmatrix} \quad (7)$$

We may derive a similar expression for Q_n , (we have to replace only j_n and j'_n in the last column of (7) by y_n and y'_n). Surface cloaking may be achieved provided that we cancel the determinants (7) for the dominant scattering orders.

III. HOMOGENIZATION THEORY FOR 3D DISPERSIVE CONFORMAL METASURFACES

Before analyzing our numerical results and confirming the possibility to cloak a spherical object with an acoustic impedance surface, we put forward a rigorous framework to homogenize acoustic conformal metasurfaces, which may be applied to a variety of geometries as quasi-periodically patterned surfaces as in Fig. 1. The model assumes that the patterns

on the surface are small compared to the wavelength, which permits an effective medium treatment of the structure. A realistic design is proposed and its cloaking capabilities are verified by full wave simulations.

The general equation governing the motion of acoustic waves is called the Lamé equation, and can be written as follows in terms of the displacement field \mathbf{u}

$$\frac{E(1-\nu)}{(1+\nu)(1-2\nu)}\nabla(\nabla\cdot\mathbf{u})-\frac{E}{2(1+\nu)}\nabla\times(\nabla\times\mathbf{u})=\rho\frac{\partial^2\mathbf{u}}{\partial t^2} \quad (8)$$

where E is the Young's modulus of the medium, ν its Poisson's ratio and ρ its density.

Let us discuss the underlying homogenization mechanism of the ultra-thin quasi-periodic acoustic spherical cloak schematized in Fig. 2 (a), which can serve as a basis for the ultra-thin cloak analyzed in section 2. For this, we resort to the von Karmann theory³² of thin elastic plates since the thickness of the metasurface is much smaller than the wavelength of sound. We note that the Lamé equation (8) can be simplified using the Helmholtz decomposition theorem with a scalar acoustic potential ϕ and a vector elastic potential $\Psi = (\Psi_1, \Psi_2, \Psi_3)$. These can be expressed in terms of the theta function Θ in the following manner:

$$\begin{aligned} \phi(x_1, x_2, x_3, t) &= \tilde{\phi}(t)\Delta\log(\Theta(x_1, x_2, x_3)), \\ \Psi_j(x_1, x_2, x_3, t) &= \tilde{\Psi}_j(t)\Delta\log(\Theta(x_1, x_2, x_3)), \end{aligned} \quad (9)$$

where $j = 1, 2, 3$. It is possible to show that the theta function is solution of the von Karmann equation^{33,34}:

$$\Lambda\nabla\cdot(\zeta^{-1}\nabla(\Delta\Lambda\nabla\cdot(\zeta^{-1}\nabla\Theta))) - \beta_0^4\Theta = 0, \quad (10)$$

where $\Lambda = \rho^{-1/2}$, $\zeta = E^{-1/2}$, with E the Young modulus of the composite constituting the ultra-thin plate cloak and $\beta_0^4 = \omega^2\rho_0 h/D_0$, with D_0 the rigidity of the cloak, $\rho_0\rho$ its density, h its thickness, and ω the pressure wave frequency.

When the pressure wave penetrates the structured ultra-thin cloak Ω whose overall geometry is shown in Fig. 2 (a), the basic cell being depicted in Fig. 2 (b), it undergoes fast periodic oscillations. To filter these oscillations, we consider an asymptotic expansion of the sequence of theta functions Θ_η solutions of Eq. (10) in terms of a macroscopic (or slow) variable $\mathbf{x} = (r, \theta, \phi)$ (in spherical coordinates, see Fig. 2) and a microscopic (or fast) variable $\mathbf{x}_\eta = (r, \theta/\eta, \phi/\eta)$, where η is a small positive real parameter.

With all the above assumptions, the theta function is solution of:

$$\rho_\eta^{-1}\nabla\cdot(\zeta_\eta^{-1}\Delta\nabla(\rho_\eta^{-1}\nabla\cdot(\zeta_\eta^{-1}\nabla\Theta_\eta))) - \beta_0^4\Theta_\eta = 0, \quad (11)$$

inside the heterogeneous isotropic ultra-thin spherical cloak Ω , where

$$\zeta_\eta = E^{-1/2} \left(\frac{\theta}{\eta}, \frac{\phi}{\eta} \right) \quad \text{and} \quad \rho_\eta = \rho^{1/2} \left(\frac{\theta}{\eta}, \frac{\phi}{\eta} \right).$$

Furthermore, $\beta_0^4 = \omega^2 \rho_0 h / D_0$, where D_0 is the flexural rigidity of the plate, ρ_0 its density and h its thickness (which are all assumed to be constant during the homogenization process i.e. they do not depend upon η).

The easiest way to handle the homogenization process is to use multiple scale techniques that amount to introducing an ansatz of the solution and a rescaling of the differential operator as follows³⁵:

$$\begin{aligned} \Theta_\eta(\mathbf{x}) &= \Theta_0(\mathbf{x}, \mathbf{x}/\eta) + \eta \Theta_1(\mathbf{x}, \mathbf{x}/\eta) + \dots, \\ \nabla &= \nabla_{\mathbf{x}} + \eta^{-1} \nabla_{\mathbf{y}} \end{aligned} \tag{12}$$

where \mathbf{x} and $\mathbf{y} = \eta^{-1} \mathbf{x}$ are respectively the slow (or macroscopic) and fast (or microscopic) variables.

In order to achieve some homogenized equation with frequency dependent parameters, we need to introduce some high-contrast in the material parameters. Similarly to what was proposed for second order partial differential equations³⁶, we further assume that

$$\begin{aligned} \zeta_\eta &= \eta^2 E_1^{-1/2} \quad \text{in inclusions and} \quad \zeta_\eta = E_2^{-1/2} \quad \text{outside inclusions,} \\ \rho_\eta &= \rho_1^{1/2} \quad \quad \quad \text{in inclusions and} \quad \rho_\eta = \rho_2^{1/2} \quad \text{outside inclusions,} \end{aligned} \tag{13}$$

where a typical pattern of high contrast inclusions is shown in Fig. 2 (a).

Using multiscale techniques for high-contrast homogenization described in³⁶, we find that the homogenized system takes the form

$$\Lambda_{hom}(\omega) \nabla \cdot ([\xi_{hom}]^{-1} \Delta \nabla (\Lambda_{hom}(\omega) \nabla \cdot ([\xi_{hom}]^{-1} \nabla \Theta_{hom}))) - \beta_0^4 \Theta_{hom} = 0, \tag{14}$$

which is the homogenized biharmonic equation with the rank-2 tensor $[\xi_{hom}]$ given by:

$$[\xi_{hom}] = \frac{E_2^{-1/2}}{\text{area}(Y^*)} \begin{pmatrix} \text{area}(Y^*) - \psi_{\theta\theta} & \psi_{\theta\phi} \\ \psi_{\phi\theta} & \text{area}(Y^*) - \psi_{\phi\phi} \end{pmatrix}. \tag{15}$$

Here Y^* denotes the region surrounding a rigid inclusion in an elementary cell of the periodic array on the surface of the ultra-thin cloak, and ψ_{ij} represent corrective terms defined by:

$$\forall i, j \in \{\theta, \phi\}, \quad \psi_{ij} = - \int_{\partial S} \Psi_i n_j \, ds, \tag{16}$$

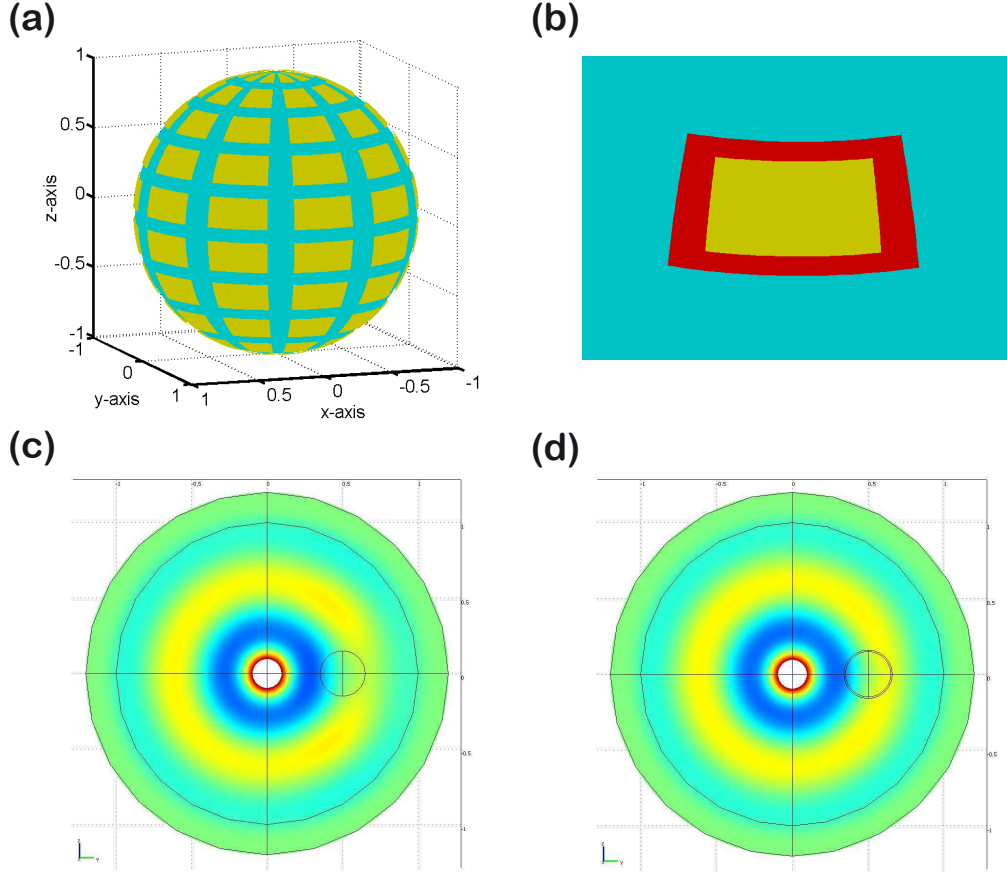


FIG. 2: (a) Schematic of the acoustic sphere to be cloaked surrounded by the patterned metasurface, the structure consists of 100 angular sectors forming a quasi-periodically surfacic phononic crystal. (b) View of the unit cell, where the annex problem defined by Eq. (17) will be solved by means of homogenization theory and leads to an effective invisibility metasurface described by Eq. (15). The total pressure field when a point source is impinging on the bare sphere (c) and the cloaked structure (an ultra-thin shell of thickness $10^{-2}a_c$ and parameters deduced from the homogenization theory was used to model the mantle cloak) (d) clearly shows the effectiveness of this mechanism for moderate sized obstacles.

where \mathbf{n} is the unit outward normal to the boundary ∂S of the inclusion on the surface of the sphere.

Furthermore, $\Psi_j, j \in \{r, \theta\}$, are periodic potentials which are unique solutions (up to an additive constant) of the following two biharmonic equations (\mathcal{K}_j):

$$(\mathcal{K}_j) : \nabla^4 \Psi_j = 0 \text{ in } Y^*, \quad (17)$$

which are supplied with the effective boundary condition $\frac{\partial \Psi_j}{\partial n} = \frac{\partial^2 \Psi_j}{\partial n^2} = \frac{\partial^3 \Psi_j}{\partial n^3} = -\mathbf{n} \cdot \mathbf{e}_j$ on the boundary ∂S of the inclusion. Here, \mathbf{e}_θ and \mathbf{e}_ϕ denote the vectors of the basis in spherical coordinates (θ, ϕ) .

It is interesting to note that the expression of the anisotropic Young's modulus has the same structure as the one of the structured plate we studied in^{37,38} in the context of cloaking for flexural waves. Somewhat more surprisingly, this homogenized Young's modulus also has the same structure as the effective shear viscosity of the structured cloak we introduced in the context of linear liquid surface waves in Ref.²⁵. However, we stress that the annex problem (17) is a bi-harmonic equation on the surface of a sphere.

Moreover, we also have some frequency dependent parameters in the homogenized equation (14).

Thus far, there is no real surprise in the model, as it has been known for over four decades that the homogenization of periodic structures brings some artificial anisotropy. However, the expression for the effective permeability is less usual:

$$\Lambda_{hom}(\omega) = \left(\int_Y \Xi(\mathbf{y}) d\mathbf{y} \right) \quad (18)$$

with $\beta(\mathbf{y})$ is the function which was first introduced in the context of high-contrast homogenization theory for second order partial differential operator by Zhikov in³⁶

$$\Xi(\mathbf{y}) = 1 + \sum_{j=1}^{\infty} \frac{\beta_0^2 E_1^{-1/2}}{\lambda_j - \beta_0^2 E_1^{-1/2}} \left(\int_Y \phi_j(\mathbf{y}) d\mathbf{y} \right)^2. \quad (19)$$

Here, λ_j and ϕ_j are the eigenvalues and orthonormal eigenfunctions of the following Laplace eigenvalue problem with homogeneous Dirichlet boundary conditions:

$$\begin{aligned} \nabla^2 v + \beta_0^2 v &= 0 \quad , \text{ in } S, \\ v &= 1 \quad , \text{ on } \partial S. \end{aligned} \quad (20)$$

The frequency dependent Zhikov's function (19) has the same features as the curves in Fig. 3, which we are now going to discuss: It tells us that the homogenized density in (14) takes some negative values near resonances of the eigenvalue problem (20).

In the present situation, we are also ensured that the homogenized pressure field within the ultra-thin cloak takes the form:

$$\phi_{hom}(x_1, x_2, x_3, t) = \tilde{\phi}(t) \Delta \log [\Theta_{hom}(x_1, x_2, x_3)] \quad , \quad (21)$$

whereby Θ_{hom} is solution of Eq. (14) if one adopts the viewpoint of plate theory as a model for pressure waves across the spherical ultra-thin cloak. Alternatively, Θ_{hom} is solution of Eq. (8). If one adopts the viewpoint of the previous section, the anisotropic density in the pressure wave equation plays the role of the anisotropic Young's modulus in (14), and the acoustic surface impedance is encompassed in the frequency dependent isotropic homogenized density in (14). Of course, these two models are ultimately equivalent, but they shed light on different aspects of the problem (volume pressure waves and surfacic metasurface cloak).

IV. NUMERICAL ANALYSIS

After having established that a rigorous homogenization approach may be applied to describe a patterned metasurface, we turn now to the numerical analysis of the surface cloaking mechanism. In Fig. 3, we show the dependency of the scattering cross-section on the surface reactance $X_s [-\mathcal{I}m(Z_s)]$ of the mantle cloak for both soft (a) and hard (c) spherical acoustic obstacles. We assume here and in the rest of this section a homogenized surface impedance, based on the results of the previous section. In what follows, we consider lossless mantle cloaks for which $R_s = \mathcal{R}e(Z_s) = 0$. We notice that due to the non-resonant nature of the mantle cloaking based on the scattering-cancellation mechanism, the scattering suppression ability is relatively robust to losses, as has been proven in the electromagnetic case¹⁸. We show also in the same plot the scattering from a bare sphere (without any cloak) for comparison (gray-dashed lines). As can be noticed from the two curves, in the limit of $X_s \rightarrow \infty$, corresponding to large reactances, the scattering tends to be that of a bare sphere and the cloak doesn't play its role of invisibility anymore. This result is not surprising and it can be understood since a large shunt reactance corresponds to the limit of no-surface. However, for a finite and broad range of values of X_s , a significant reduction of scattering is achieved, for different values of a_c (radius of the cloak) as can be seen in Fig. 3 (a) and (c), even in the limit of a conformal cloak ($a_c = a$).

To further demonstrate the validity of our approach to surface cloaking we now analyze the frequency response of the cloak. This can be seen in Fig. 3 (b) and (d) that correspond respectively to Fig. 3 (a) and (c), with $a_c = a$ (conformal) and $a_c = 1.1a$. For these simulations, we have made the assumption that the surface reactance does not depend on

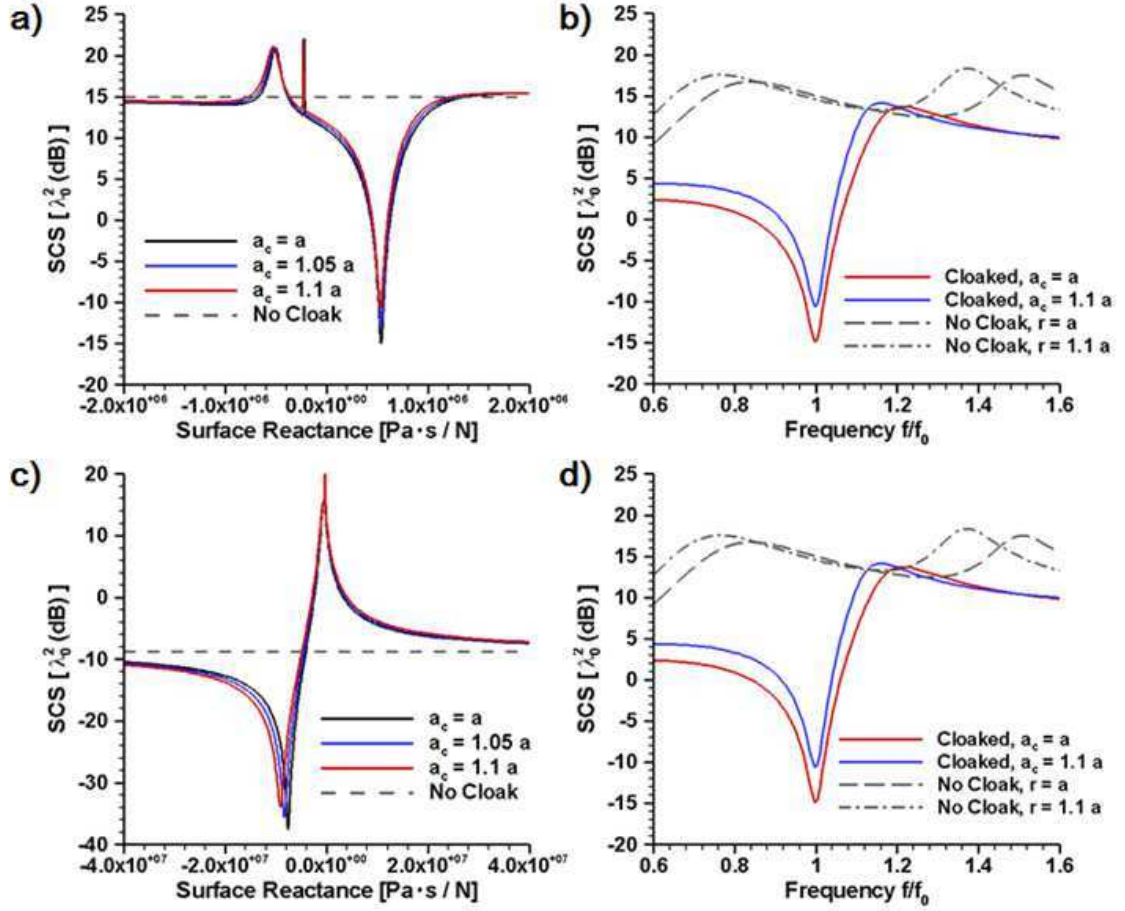


FIG. 3: Dependencies of the total SCS of a spherical obstacle with $2a = \lambda_0/5$ and $\kappa_r = 1/10$ on (a) the reactance of the mantle cloak and (b) the normalized frequency of operation for different ratios of a/a_c . (c) and (d) are similar to (a) and (b), but for a spherical obstacle with comparable size and $\kappa_r = 10$, where κ_0 denotes the bulk modulus of the surrounding medium and is taken equal to 1.

frequency over the range of interest (which is a fair approximation in a variety of acoustic scenarios). By comparing the uncloaked case with the cloaked one, it is evident that an excellent scattering reduction may be achieved over a finite range of frequencies for hard and soft obstacles.

Finally, we perform a numerical analysis of the field scattered by a plane acoustic wave vibrating harmonically. A plane wave is incident from top to bottom and encounters the

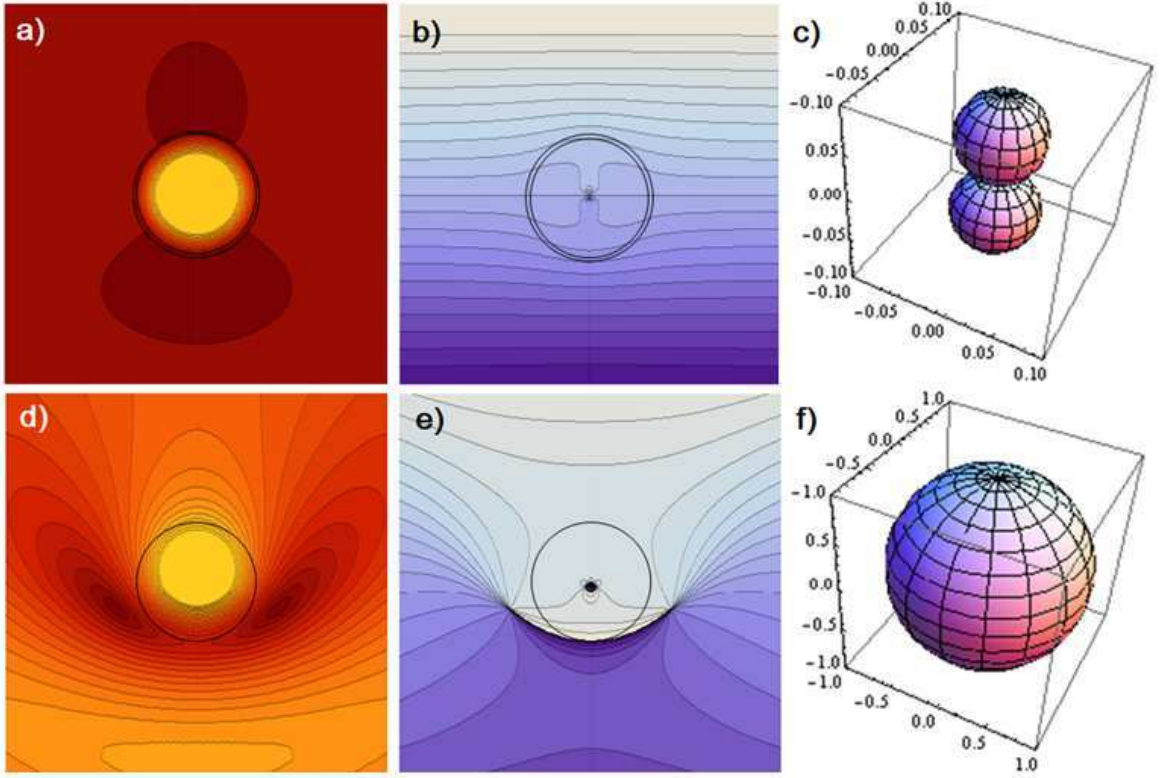


FIG. 4: Amplitude of the pressure field on the x - y plane for a spherical obstacle with $2a = \lambda_0/5$ and $\kappa = 1/10$ (a) with and (d) without the mantle cloak. (b) and (e) are similar to (a) and (d), but for the phase of the pressure field on the orthogonal x - z plane. (c) and (f) are the associated normalized far-field scattering patterns (the cloaked scenario are two orders of magnitude lower than the uncloaked one).

spherical obstacle (for the two scenarios of cloaked and uncloaked sphere). Figures 4 and 5 show simulations for respectively hard and soft obstacles with radius $2a = \lambda_0/5$, where λ_0 is the wavelength of the incident wave.

For example Fig. 4 (d) and (e) show the pressure field amplitude for two orthogonal planes of phase (x - y and x - z) and show the distortion of the field due to strong scattering by the obstacle. Figures 4 (a) and (b) show the phase for the same obstacle when it is cloaked and, as expected, the field outside the cloak is identical to the one we obtain when we have free-space (homogeneous medium without any obstacle). This shows the efficiency of cloaking by surface impedance.

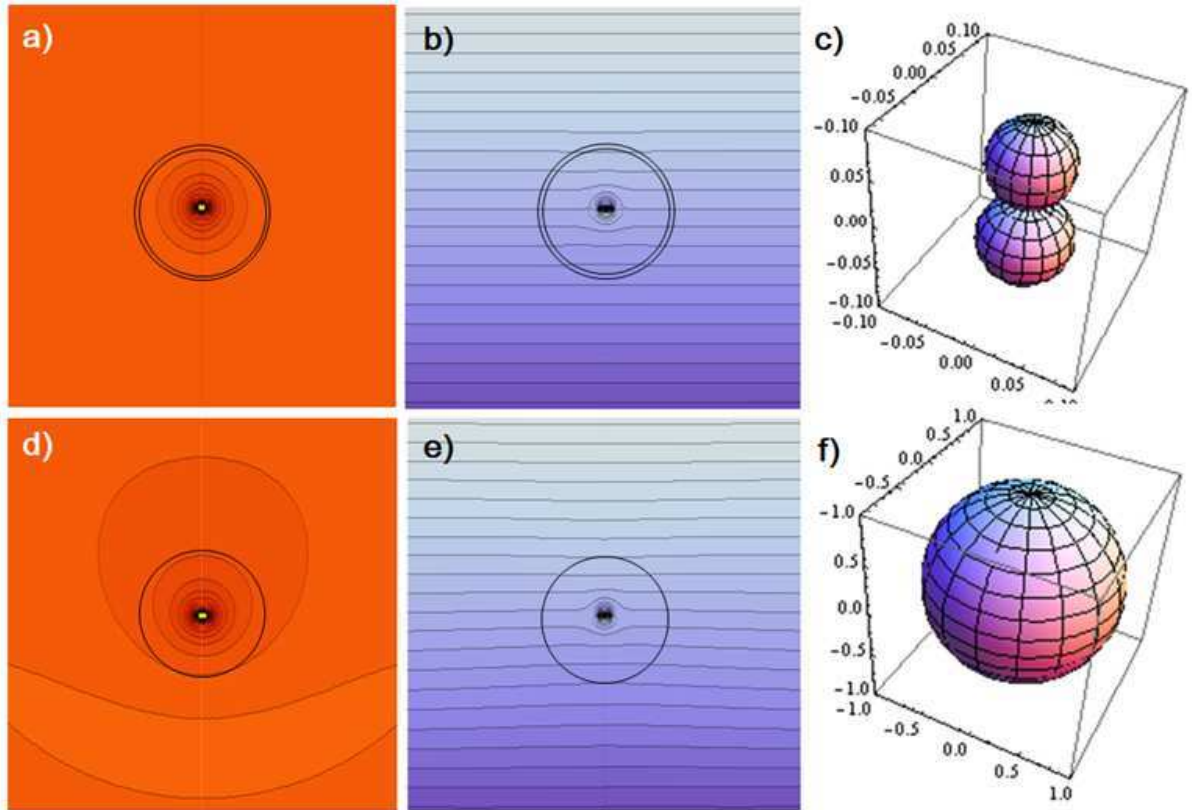


FIG. 5: Similar to Fig. 3, but for a spherical obstacle with $2a = \lambda_0/5$ and $\kappa = 1/10$.

To further check the functionality of our cloak, we show on Fig. 4 (c) and (f) [and Fig. 5 (c) and (f)] the scattering diagrams computed in the far-field for both the cloaked and uncloaked object. It is obvious that the cloaked obstacle is nearly invisible. [One should take into account the difference in the upper axis limits between Fig. 4,5 (c) and (f)].

V. CONCLUSION

In conclusion, we have studied analytically and numerically the extension of the cloaking mechanism described in Ref.¹⁸ to the domain of 3D spherical acoustic waves. We have shown numerically that a surface impedance cloaking device is possible, provided we choose a convenient reactance to reduce drastically the scattering from a spherical shaped obstacle. Importantly, numerical results are supplied with a homogenization model which gives the effective parameters of 3D conformal surfaces. We believe that our results make the cloaking theory one step closer to its practical realization for acoustic waves since the proposed device

is a lot more thinner and lighter than its classical bulk counterparts. This mechanism could also be used to build non-invasive sensing devices (e.g. ultrasound imaging) with moderately broadband features.

Last but not least, we would like to point out that the techniques developed in this paper for pressure waves in fluids can be extended to flexural waves in plates, in which case applications shift towards suppression of unwanted mechanical vibrations in aeronautic, ship or car components. On a larger scale, one should note that fourth-order and higher order governing equations as those described in Section 3 are a good asymptotic model for Rayleigh waves propagating at the surface of the Earth: ultra-thin mantle cloaks could therefore open new concepts in seismic cloaks.

* Equal contribution: `mohamed.farhat@fresnel.fr`

† Equal contribution: `pychen@utexas.edu`

‡ Electronic address: `alu@mail.utexas.edu`

¹ J.B. Pendry, D. Schurig, and D.R. Smith, *Science* **312**, 1780-2 (2006).

² D. Schurig, J.J. Mock, J.B. Justice, S.A. Cummer, J.B. Pendry, A.F. Starr, and D.R. Smith, *Science* **314**, 977-80 (2006).

³ U. Leonhardt, *Science* **312**, 1777-80 (2006).

⁴ U. Leonhardt and T. G. Philbin, *New J. Phys.* **8**, 247 (2006).

⁵ J.B. Pendry, *Phys. Rev. Lett.* **85**, 3966 (2000).

⁶ N.A. Nicorovici, R.C. McPhedran, and G.W. Milton, *Phys. Rev. B* **49**, 8479-8482 (1994).

⁷ N.A.P. Nicorovici, G.W. Milton, R.C. McPhedran, L.C. Botten, *Opt. Express* **15**, 6314-6323 (2007).

⁸ W. Cai, U.K. Chettiar, A.V. Kildiev, and V.M. Shalaev, *Nat. Photon.* **1**, 224-227 (2007).

⁹ M. Farhat, S. Guenneau, A.B. Movchan, and S. Enoch, *Opt. Express* **16**, 5656-5661 (2008).

¹⁰ A. Alù, and N. Engheta, *Phys. Rev. E* **72**, 016623 (2005).

¹¹ A. Alù, and N. Engheta, *Phys. Rev. Lett.* **102**, 233901 (2009).

¹² A. Alù, and N. Engheta, *Phys. Rev. Lett.* **105**, 263906 (2010).

¹³ B. Edwards, A. Alù, M. G. Silveirinha, and N. Engheta, *Phys. Rev. Lett.* **103**, 153901 (2009).

¹⁴ D. Rainwater, A. Kerkhoff, K. Melin, J. C. Soric, G. Moreno, and A. Alù, *New J. Phys.* **14**,

- 013054 (2012).
- ¹⁵ S. Mühlig, M. Farhat, C. Rockstuhl, and F. Lederer, Phys. Rev. B **83**, 195116 (2011).
- ¹⁶ A. Monti, F. Bilotti, and A. Toscano, Opt. Lett. **36**, 4479 (2011).
- ¹⁷ Y.I. Bobrovnikskii, New J. Phys. **12**, 043049 (2010).
- ¹⁸ A. Alù, Phys. Rev. B **80**, 245115 (2009).
- ¹⁹ P.Y. Chen, and A. Alù, IEEE Int. Sym. Antennas and Propagat., Toronto, Canada, July 11-17 (2010).
- ²⁰ P.Y. Chen, and A. Alù, ACS Nano **05**, 5855-5863 (2011).
- ²¹ P.Y. Chen, and A. Alù, Phys. Rev. B **84**, 205110 (2011).
- ²² B.A. Munk, *Frequency selective surface: theory and design*, (John Wiley and Sons, New York, 2000).
- ²³ S.A. Cummer and D. Schurig, New J. Phys. **9**, 45 (2007).
- ²⁴ D. Torrent and J. Sanchez-Dehesa, New J. Phys. **10**, 063015 (2008).
- ²⁵ M. Farhat, S. Enoch, S. Guenneau and A.B. Movchan, Phys. Rev. Lett. **101**, 134501 (2008).
- ²⁶ H. Chen and C. T. Chan, Appl. Phys. Lett. **91**, 183518 (2007).
- ²⁷ S.A. Cummer, B.I. Popa, D. Schurig, D.R. Smith, J. Pendry, M. Rahm, and A. Starr, Phys. Rev. Lett. **100**, 024301 (2008).
- ²⁸ M.D. Guild, M.R. Haberman, and A. Alù, Wave Motion **48**, 468-482 (2011).
- ²⁹ M.D. Guild, A. Alù, and M.R. Haberman, J. Acoust. Soc. Am. **129**, 1355-1365 (2011).
- ³⁰ P.-Y. Chen, M. Farhat, S. Guenneau, S. Enoch, and A. Alù, Appl. Phys. Lett. **99**, 191913 (2011).
- ³¹ J. J. Bowman, T. B. A. Senior, and P. L. E. Uslenghi, *Electromagnetic and Acoustic Scattering by Simple Shapes* (Harper Row, London, 1987).
- ³² K.F. Graff, *Wave motion in elastic solids* (Dover, New York, 1975).
- ³³ J. Kapelewski and J. Michalec, Int. J. Eng. Sci. **29**, 285-91 (1991).
- ³⁴ L. Munteanu and V. Chiroiu, New J. Physics **13**, 083031 (2011).
- ³⁵ A. Bensoussan, J.L. Lions, G. Papanicolaou, *Asymptotic analysis for periodic structures* (North-Holland, Amsterdam, 1978).
- ³⁶ V.V. Zhikov Sbornik: Mathematics **191**, 973-1014 (2000).
- ³⁷ M. Farhat, S. Guenneau and S. Enoch, Phys. Rev. Lett. **103**, 024301 (2009).
- ³⁸ M. Farhat, S. Guenneau and S. Enoch, Phys. Rev. B **85**, 020301(R) (2012).